

# Theory of Parallel MRI and Cartesian SENSE Reconstruction: Highlight

Joseph Suresh Paul, Raji Susan Mathew and M.S. Renjith

**Abstract** Magnetic resonance imaging (MRI) is a well-known medical imaging technique, that exclusively uses the response of the hydrogen nucleus which is abundant in the human body. In recent years, parallel MRI techniques have been developed to accelerate image acquisition. A notable development in parallel MRI was the introduction of SMASH by Sodicksen and Manning. Since then, great progress in the development and improvement of parallel imaging reconstruction methods has taken place. The Sensitivity Encoding (SENSE) proposed by Preussmann and Weiger is the most widely used image-domain parallel MR image reconstruction technique. SENSE uses an initial estimate of the coil sensitivity in combination with an SNR optimized noise inversion to obtain the final reconstructed image. This chapter starts with a brief history of the parallel imaging, discusses the estimation of sensitivity and SENSE reconstruction.

## 1 Introduction to Parallel Imaging

Magnetic resonance imaging (MRI) is a well-known medical imaging technique that exclusively uses the response of the hydrogen nucleus which is abundant in the human body [1]. Variation of hydrogen density and specifically its molecular binding in different tissues produces a much better soft tissue contrast than CT. MRI has some further advantages if compared with x-ray and CT: (i) MRI does not use ionizing radiation. (ii) Images can be generated with arbitrary slice orientation including coronal and sagittal views. (iii) Several different functional attributes can be imaged with MRI. (iv) Capability to provide risk-free diagnostic assessment. However, rapid switching of magnetic field gradients often causes severe discomfort to the subject being scanned. This forms a serious impediment requiring

---

J.S. Paul (✉) · R.S. Mathew · M.S. Renjith  
Medical Image Computing and Signal Processing Laboratory,  
Indian Institute of Information Technology and Management-Kerala,  
Thiruvananthapuram, India  
e-mail: j.paul@iiitmk.ac.in

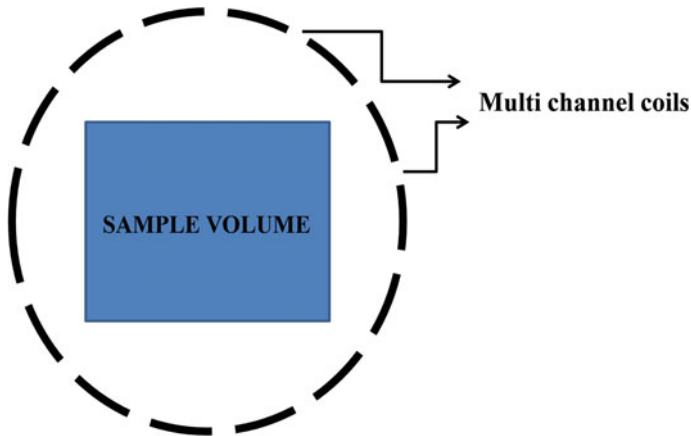


**Fig. 1** Schematic representation of parallel imaging

scanning protocols to be implemented in a shorter period of time, simultaneously maintaining the image quality. Imaging speed is a crucial consideration for magnetic resonance imaging (MRI). The speed of conventional MRI is limited by hardware performance and physiological safety measures. In the recent years, parallel MRI techniques have been developed that utilize radiofrequency (RF) coil arrays to accelerate image acquisition beyond these previous limits [2–10].

“Parallel” MRI is a new technique that circumvents these limitations by utilizing arrays of radio frequency detector coils to acquire data in parallel, thereby enabling still higher imaging speeds. In parallel MRI, coil arrays are used to accomplish part of the spatial encoding that was traditionally performed by magnetic field gradients alone. A schematic representation of parallel MRI is given in Fig. 1. The term parallel imaging comes from the fact that signals are acquired simultaneously from multiple coils. The effective use of multiple coils in parallel has been shown to multiply imaging speed, without increasing gradient switching rate or RF power deposition. In parallel imaging, the acquisition is speeded up by under-sampling the data received from the multiple coils. Under-sampling is described by factor called acceleration factor. The resulting data loss and consequent aliasing is compensated by the use of additional spatial information obtained from several receiver coils.

Spatial localization in conventional MRI is accomplished using a set of magnetic field gradients. The spatially varying fields resulting from the application of each gradient pulse spatially encodes the received signal, and generates an image using Fourier approximation. In conventional MR acquisition, the Fourier space is scanned line-by-line [11, 12]. This considerably limits the speed of image acquisition. Protocols with delayed scan times are not desirable, particularly for imaging applications involving repeated acquisitions. This includes functional imaging, perfusion and diffusion imaging, and imaging of the beating heart. Even though methods are available for tracking motion [13, 14], or reduction of accompanying

motion induced artifacts [15], accelerated MRI provides better solution for above applications.

Parallel MRI (pMRI) uses spatially separated receiver coils to perform spatial encoding. Though the theoretical foundation of pMRI was established in 1980s [16], not much was done in terms of its implementation due to the inability to design parallel coils capable of providing high Signal-to-Noise Ratio (SNR) images in a large enough Field Of View (FOV). Due to this, several attempts were made to accelerate MR acquisition using alternate means such as minimization of TR (Repetition Time) by increasing the gradient strength, and single shot imaging [17]. However, the performance of above methods was limited by the allowable strength of gradient pulse amplitudes. The idea of using phased array coils for MRI dates back to the early eighties, wherein the design efforts were largely concentrated in building array coils with reduced coil-to-coil coupling [18, 19]. The phased array coils are beneficial due to their ability to generate high SNR signals with reduced motion artifacts. The first phased array MRI system implemented by Roemar et al. [20] in the form of two inductively coupled resonant rings, electrically isolated from each other with a decoupling element connected between the rings. In this, differential weighting of signals from the two coils were used for signal localization, thereby reducing the need for time consuming gradient-encoding steps. Enhancement of SNR was achieved by means of the decoupling circuitry. For  $n_c$  independent coils in the absence of mutual coupling, the SNR is increased by a factor of square root of  $n_c$ . A detailed description of phased-array MRI technology is provided in the review article [21]. Recent advances in the design of MRI equipment and imaging procedures is described in [22].

In conventional MR imaging, the phase-encoding steps are performed in sequential order by switching the magnetic field gradient step-by step, which in turn determines the speed of acquisition. Since the switching is expensive, acceleration is achieved by skipping alternate phase encoding lines. This was first implemented in 1989 by under sampling the k-space in PE (Phase Encode) direction [23]. Since SNR is dependent on the number of phase encoding steps used, accelerated image acquisition can be achieved only at the expense of reduction in SNR. However, the reduced SNR is compromised by elimination of phase related distortion. Irrespective of the MRI sequence used, parallel imaging maintains image contrast without need for higher gradient system performance.

We now come to the question of how parallel MRI makes imaging faster. Assume the number of voxels, the number of receiver channels, the number of frequency encoding steps and the number of phase encoding steps are  $n_v$ ,  $n_c$ ,  $N_{fe}$  and  $N_{pe}$ , respectively. Obviously, the number of measured samples is  $n_c \times N_{fe} \times N_{pe} = n_c \times n_k = N_s$  (where  $n_k$  is the number of sampling positions in k-space). To make reconstructions feasible, it is necessary that

$$N_s \geq n_v \quad (1)$$

In conventional single channel MRI,  $N_s = N_{fe} \times N_{pe} = n_v$ . For example, to obtain a  $256 \times 256$  image, the acquisition matrix is also  $256 \times 256$ . In parallel MRI, since

$n_c > 1$ , it is possible that we reduce the number of frequency encoding or phase encoding steps while still having enough information for a feasible reconstruction. Usually, the k-space is evenly under-sampled in the phase encoding direction to reduce the scanning time. The rate at which under-sampling is performed is called acceleration factor or acceleration rate [3, 4]. An obvious implication of Eq. (1) is that the largest possible acceleration rate is equal to the number of channels.

In summary, if an array of RF coils is used to acquire MR signals simultaneously and the coil sensitivities are available, the spin density may be determined from a reduced set of phase encodings. This is the basic principle of parallel imaging.

## 2 Background

### 2.1 History of Parallel Imaging Methods

The performance of pMRI is largely determined by the coil geometry. For instance, large coils cover large areas of the subject, resulting in low SNR due to small fraction of the sensitive volume occupied by the sample. The coil sensitivity can be considered as a point spread function that serves to degenerate the received signal, in addition to the additive noise. However, the spatial sensitivity profiles of each receiver coil serve to provide an additional encoding in pMRI. Better image reconstruction becomes possible only with prior knowledge of the coil sensitivities.

The first step towards pMRI was proposed by Carlson [16] in 1987. His method consisted of a uniform sensitivity pattern in one coil while applying linear gradient in the other. In this fashion, a Fourier series expansion was used to reconstruct the unfolded image data in k-space. Kelton et al. [22] proposed a second method of reconstruction in the spatial domain, wherein a matrix inversion was employed to unalias the image. Subsequently, this method was further modified to include reduction factors greater than two, but less than the number of coils used [2]. Theoretically, imaging time reduces by number of array coils, but practically lesser due to sensitivity noise, and increased coupling between coils. The basic limitation for all the above studies was the need for a reliable method to determine the individual coil sensitivity function.

A notable development following this period was the introduction of Simultaneous Acquisition of Spatial Harmonics (SMASH) method by Sodickson and Manning [3]. SMASH is the first experimentally successful parallel imaging technique that uses linear combinations of coil sensitivity profiles to generate low-order spatial harmonics of the desired FOV. Sodickson and Griswold then presented a successful in vivo implementation of pMRI using the SMASH technique, thereby starting the rapidly growing field of parallel imaging [24]. Only one year later, Pruessmann and Weiger proposed the concept of sensitivity encoding (SENSE) [3] which is strongly related to the early proposals of Kelton [23], Ra and Rim [2]. The difference between the two is that SENSE uses an SNR optimized

matrix inversion in combination with an initial estimate of the coil sensitivity mapping. Since then, great progress in the development and improvement of parallel imaging reconstruction methods has taken place, thereby producing a multitude of different and somewhat related techniques and strategies [3–5, 9, 10, 24–26]. Currently, the best-known are SMASH [3], SENSE [4] and GRAPPA [9]. However, various other techniques, such as AUTOSMASH [25], VD-AUTO-SMASH [26], Generalized SMASH [10], mSENSE [27], PILS [6] and SPACERIP [5] have also been proposed.

## 2.2 Spatial Encoding and Image Reconstruction

The general equation of multi-channel MR acquisition can be expressed as

$$s_l(k_x, k_y) = \iint_{xy} C_l(x, y) \rho(x, y) e^{-i2\pi(k_x x + k_y y)} dx dy \quad (2)$$

where  $C_l(x, y)$  denotes the coil sensitivity profile of the  $l$ th channel [28]. Here, the signal comprises an integration of the spin density  $\rho(x, y)$  against the spatial encoding function consisting of coil sensitivity and gradient modulation. Unlike Fourier encoding where off-resonance frequencies are determined in accordance with spatial positions, the sensitivity encoding functions serve to differentially sample the image based on the spatial positions closer to the respective coils. These functions may be regarded as representing different “views” or “projections” of the image to be reconstructed, with each measured signal point representing the appearance of the image from the corresponding perspective, as illustrated in Fig. 2.

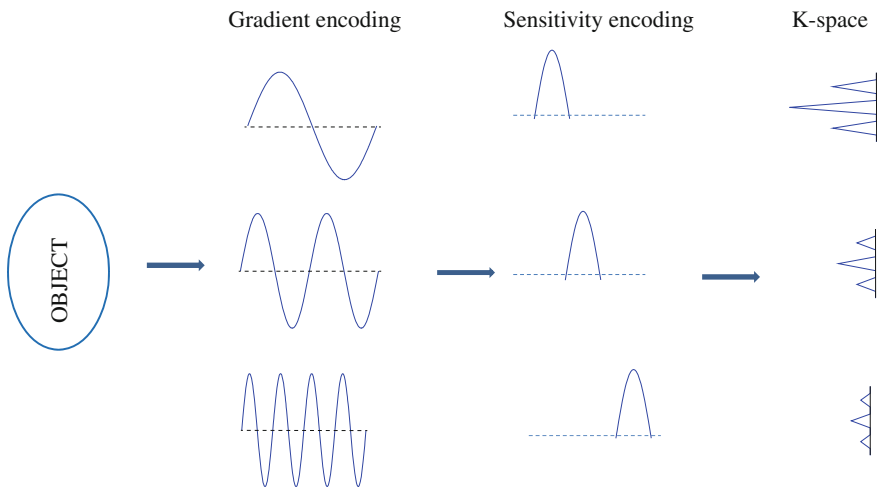


**Fig. 2** Encoding scheme in pMRI

In multi-channel acquisition, the received signal in each coil is weighted by the coil sensitivity function  $C_l(r)$ , and the magnetic field  $B(r)$ . In terms of the weighting functions, the spatial encoding function of MR acquisition can be expressed as

$$E_\zeta(r) = \frac{\gamma^2 \hbar}{4k_B T} C_l(r) B(r) e^{-i\gamma[B(r)-B_0]t} \Big|_{t=t_\zeta} \quad (3)$$

The discrete time measured signal can be generalized to be the inner product

$$s_\zeta = \langle E_\zeta(r), \rho(r) \rangle \quad (4)$$

For a k-space with  $N$  points, the basis vectors then produce a signal vector with  $N$  elements

$$s = \begin{bmatrix} s_1 \\ s_2 \\ \bullet \\ \bullet \\ \bullet \\ s_N \end{bmatrix} = \begin{bmatrix} \langle E_1(r), \rho(r) \rangle \\ \langle E_2(r), \rho(r) \rangle \\ \bullet \\ \bullet \\ \bullet \\ \langle E_N(r), \rho(r) \rangle \end{bmatrix} \quad (5)$$

For each discretized location  $r$ , Eq. (5) can be represented in the matrix form

$$s = E\rho \quad (6)$$

where  $s$  and  $\rho$  contain the measured samples and image pixels, respectively.  $E$  is referred to as the generalized encoding matrix (GEM) [8] with dimension  $N_s \times n_p$ . Equation (6) shows that the encoding of MRI is essentially a linear transform, and the reconstruction in general involves inverse problems, namely,

$$\hat{\rho} = E^{-1}s \quad (7)$$

The major difficulty is that the dimension of the GEM  $E$ , is in general, rather large and direct inversion is prohibitively time-consuming and memory-intensive. The inversion operation is simplified using different pMRI reconstruction methods. In further discussions, the number of voxels, the number of receiver channels, the number of frequency encoding steps and the number of phase encoding steps are denoted by  $n_v$ ,  $n_c$ ,  $N_{fe}$  and  $N_{pe}$ , respectively. Obviously, the number of measured samples will be  $n_c \times N_{fe} \times N_{pe} = n_c \times n_k = N_s$  (where  $n_k$  is the number of sampling position in k-space) and the encoding matrix  $E$  is of dimension  $N_s \times n_v$ . To make reconstructions feasible, it is necessary that  $N_s \geq n_v$ .

### 2.3 Sensitivity Calibration to Obtain the Encoding Matrix $E$

At a given sampling location, the encoding function and coil sensitivity are related in the form

$$E_{k,l}(r) = \frac{\gamma^2 \hbar^2}{4k_B T} C_l(r) e^{ik \cdot r} \quad (8)$$

The coil sensitivities are calculated from the knowledge of coil array geometry. For flexible coil arrays, the coil sensitivity functions are to be recalibrated due to scan-to-scan changes in the coil locations. The coil modulated images are given by

$$\rho_l(r) = C_l(r) \rho(r) \quad (9)$$

The coil images have a non-uniform intensity distribution due to the spatially varying sensitivity values. Meaningful information about the image can only be obtained once the individual coil images are combined so as to have a uniform spatial sensitivity  $C_0$  at all spatial location. The uniform spatial profile is obtained in practice by using a bird-cage body coil. The ratio of channel image to the body coil image, therefore, yields

$$\frac{\rho_l(r)}{\rho_{body-coil}(r)} = \frac{C_l(r)}{C_0} \quad (10)$$

Alternatively, a sum-of-squares combination yields

$$\frac{\rho_l(r)}{\sqrt{\sum_l |\rho_l(r)|^2}} = \frac{C_l(r)}{\sqrt{\sum_l |C_l(r)|^2}} \quad (11)$$

Since the multiplication of  $\frac{1}{\sqrt{\sum_l |C_l(r)|^2}}$  is common to all coils, it can be incorporated in the formulation of an effective encoding function which differs from the original encoding Eq. (8) as follows:

$$\tilde{E}_{k,l}(r) = \frac{E_{k,l}(r)}{\sqrt{\sum_l |C_l(r)|^2}} \quad (12)$$

All pMRI methods effectively reconstruct the image  $\tilde{\rho}(r)$  given by

$$\hat{\rho}(r) = \sqrt{\sum_l |C_l(r)|^2} \rho(r) \quad (13)$$

Calibration data, used to reconstruct the coil images can be obtained from a separate scan before or after the image acquisition. Because of the requirement of external information, this approach is generally known as external calibration. Alternatively, the calibration scan can be incorporated as a part of the image acquisition, and the calibration data can be extracted from the image dataset. This approach is called auto-calibration or self-calibration. The crucial difference between the external- and self-calibration approaches lies in the timing of the acquisition of calibration data relative to the image acquisition.

SENSE reconstruction methods require a prior knowledge of the coil sensitivity profiles. The SENSE method is mathematically an exact reconstruction method proposed by Pruessmann et al. [4]. SENSE is the most popular image-space based pMRI technique, which is being offered by many companies particularly Philips (SENSE), Siemens (mSENSE), General Electric (ASSET), and Thoshiba (SPEEDER). SENSE is the most used pMRI method for clinical applications due to its broad availability and the enhanced image acquisition capabilities.

The SENSE method addresses the most general case of combined gradient and sensitivity encoding. The two reconstruction approaches in SENSE include strong reconstruction for optimal voxel shape and weak reconstruction for approximate voxel shape using Dirac function [4] accompanied by SNR reduction. The reconstruction algorithm for both the approaches are numerically demanding due to the hybrid encoding nature. Use of FFT (Fast Fourier Transform) is possible only in the case of weak reconstruction for Cartesian SENSE.

### 3 SENSE Methods

#### 3.1 Representation of Aliased Images

For achieving scan time reduction in pMRI, phase encoding lines are under-sampled by an acceleration factor  $R$ . Therefore, the distance between phase encoding lines is increased by  $R$ . Even though number of phase encoding steps  $N_{pe}$  is reduced, the maximum gradient strength  $N_{pe} \times G_y$  remains same. This results in aliased image reconstruction. The k-space  $s'_i$  retrieved with an acceleration factor  $R$  is identical to complete k-space  $s_i$  excluding the unacquired lines. The FOV is reduced only in the phase encoding direction, because the 2D Fourier transformation is separable. The aliased image is obtained by an inverse Fourier transformation of  $s'_i$  in  $y$  direction.



$$\begin{aligned}
\rho_l^r(x, y) &= DFT_y^{-1} \{s_l^r(x, k_y)\} \\
&= \frac{R}{N_{pe}} \sum_{k_y=0, R, 2R, \dots}^{N_{pe}-R} s_l(x, k_y) e^{ik_y y} \\
&= \frac{R}{N_{pe}} \sum_{k_y=0, R, 2R, \dots}^{N_{pe}-R} e^{ik_y y} \sum_{y'=0}^{N_{pe}-1} \rho(x, y') e^{-ik_y y'} \\
&= \frac{R}{N_{pe}} \sum_{y'=0}^{N_{pe}-1} \rho(x, y') \sum_{k_y=0, R, 2R, \dots}^{N_{pe}-R} e^{ik_y y} e^{-ik_y y'} \\
&= \frac{R}{N_{pe}} \sum_{y'=0}^{N_{pe}-1} \rho(x, y') \sum_{k_y=0, 1, 2, \dots}^{\frac{N_{pe}}{R}-1} e^{ik_y y} e^{-ik_y y'}
\end{aligned} \tag{14}$$

Since  $e^{ik_y y}$  and  $e^{-ik_y y'}$  are orthogonal, the sum over  $k_y$  for  $R = 1$  gives zero for all  $y \neq y'$ .  $\frac{R}{N_{pe}}$  is assumed to be an integer for simplicity. For  $R > 1$  the exponential functions can be represented as the sum of  $R$  Kronecker delta functions.

$$\begin{aligned}
\rho_l^r(x, y) &= \sum_{y'=0}^{N_{pe}-1} \sum_{m=0}^{R-1} \delta(y', y \bmod \frac{N_{pe}}{R} + m \times \frac{N_{pe}}{R}) \rho(x, y') \\
&= \sum_{m=0}^{R-1} \rho(x, y \bmod \frac{N_{pe}}{R} + m \times \frac{N_{pe}}{R})
\end{aligned} \tag{15}$$

Each value in aliased image  $\rho_l^r$  is a superposition of  $R$  values from the original image.

### 3.2 SENSE Reconstruction Using Encoding Matrix Formulation

The ideal image  $\rho$  and k-space values  $s_l(k_x, k_y)$  are related using the encoding matrix  $E$ .

$$s_l(k_x, k_y) = \sum_{k_x, k_y} \rho(x, y) E_{l, k_x, k_y}(x, y) \tag{16}$$

where the encoding matrix  $E$  is

$$E_{l, k_x, k_y}(x, y) = e^{-i\pi(k_x x + k_y y)} C_1(x, y) \tag{17}$$

The image reconstruction is performed using the linear reconstruction matrix  $F$

$$\hat{\rho}(x, y) = \sum_{l, k_x, k_y} F_{l, k_x, k_y}(x, y) s_l(k_x, k_y) \quad (18)$$

The reconstruction matrix  $F$  is estimated using weak voxel criterion, where the voxel functions are approximated using Dirac function. The  $F_{[x, y; l, k_x, k_y]}$  and  $E_{[l, k_x, k_y; x, y]}$  related by

$$FE = \text{Id}_{n_v} \quad (19)$$

where  $\text{Id}_{n_v}$  is an  $n_v \times n_v$  identity matrix. Equation (19) is valid only under ideal conditions when the data is fully sampled and the receiver coils have no overlap. However, the latter condition is not fully valid for phased arrays for which the relation between reconstruction and encoding matrices are determined by a sample noise matrix. A detailed discussion of these effects are presented in the next section.

### 3.3 Phased Arrays

One of the basic requirement of parallel MRI is to acquire MR signals simultaneously using multiple coil elements from a receiver coil array. The coil arrays are conventionally called “phased array”, had been invented and widely used in MRI even before the advent of parallel imaging. It was developed in 1990 by Roemer [29], improve SNR for large FOV applications.

The concept of phased array was first introduced in phased array radar and ultrasound. In an array data is acquired simultaneously and combined subsequently from a multitude of closely positioned receive coils so that SNR and resolution of small surface coils can be obtained over a large FOV normally associated with body imaging with no increase in imaging time. An important issue compared to the design of a single surface coil is that there may be interactions among nearby coil elements, commonly called “mutual coupling”. To minimize the coupling effect various techniques, such as overlapping [29], low impedance preamplifier [29], interconnecting capacitors/inductors have been proposed.

Figure 3a shows a schematic of a 4-element phased array using Shepp-Logan phantom image. Each receiver acquires MR signals independently. The absolute magnitude single-coil images from the four channels are displayed in Fig. 3b. It is shown that for each channel, high SNR is observed in a certain region of the FOV; after combination, it is expected that we can obtain high SNR over the entire FOV. The data combination algorithms are discussed as follows.

For an  $N$ -element phased array, let  $Y$  denote the  $N \times N$  receiver noise matrix, with the  $m$ -th entry representing noise correlation between the  $m$ th and the  $n$ th channel, and the  $m$ th diagonal element representing the noise level of the  $m$ th

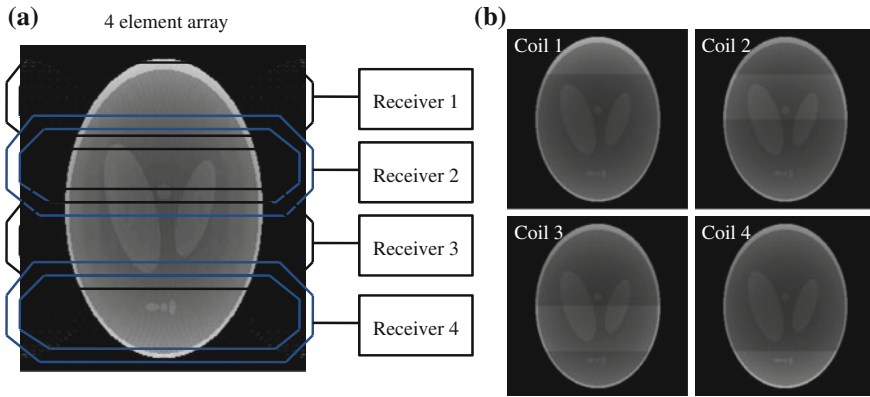


**Fig. 3** **a** Schematic of a phased array coil using Shepp-Logan, **b** Absolute magnitude single-coil images from the four channels

channel. For a given point  $(x, y)$ , let  $p_i$  denote the pixel value from the  $i$ th channel and  $P = [p_1 \ p_2 \ p_3 \ \dots \ p_N]^T$ , let  $c_i$  denote the complex sensitivity of the  $i$ th coil at that point and  $C = [c_1 \ c_2 \ c_3 \ \dots \ c_N]$ . The combined pixel value with optimized SNR, according to [19], is expressed as

$$p_{\text{combine}} = \lambda P^T \Psi^{-1} C \tag{20}$$

where  $\lambda$  is a constant scaling factor. The optimum data combination can be obtained as a linear combination of data from individual channels with appropriate weightings to each position. When the noise correlation is negligible, it is easily shown that the SNR-optimized composite image is a combination of single-coil images weighted by their respective sensitivities.

The accurate knowledge of sensitivity is required to combine the data as shown in Eq. (20). Since in some cases, measuring the sensitivity of each coil is excessive, it is desirable to have a technique which combines the data without detailed knowledge of the coil sensitivity while at the same time preserves high SNR. For this purpose, the coil sensitivities in Eq. (3) are approximated by the single-coil images themselves. This leads to the more commonly used “sum-of squares” combination [29], which takes a simpler form

$$p_{\text{combine}} = \sqrt{P^H P} \tag{21}$$

where the superscript  $H$  denotes conjugate transpose.

If the different coils have a significant overlap, the matrix inversion in Eq. (7) is challenging because the rows of the sensitivity matrix  $C_1$  becomes linearly dependent. This leads to noise amplification in the reconstructed image. The noise arises due to the reduced amount of acquired data. Due to the mutual coupling between coils, this noise is spatially varying. The spatial variation in noise is

quantified using a noise covariance matrix. With  $\mathbf{p}_p$  representing a vector consisting of signals  $\rho_{1,p}$  from the same location in each coil element, SNR of the Root Sum-of-Squares (RSoS) image is expressed as

$$\text{SNR}_{\text{RSoS}}(\mathbf{p}) = \sqrt{\mathbf{p}_p^H \boldsymbol{\Psi}^{-1} \mathbf{p}_p} \quad (22)$$

where  $\boldsymbol{\Psi}$  denotes the noise covariance matrix, that is approximated by summing the scalar dot product of coil sensitivities over a number of points. The  $(i, j)$ th element of this matrix is obtained as

$$\Psi_{i,j} = \sum_{p=1}^{n_v} C_i(p) \cdot C_j(p), \quad \text{for } i, j = 1, 2, \dots, n_c. \quad (23)$$

The  $\boldsymbol{\Psi}$  is the  $n_c \times n_c$  receiver noise matrix which denotes the variance in each coil as well as correlation between coils. The propagation of noise from k-space to image-space is described by the sample noise matrix  $\tilde{\boldsymbol{\Psi}} = \boldsymbol{\Psi} \otimes Id_{n_k}$  and image noise matrix  $X$  in which the  $p$ th diagonal element represents the noise variance in the  $p$ th image value and off-diagonal elements provides noise correlation between image values. The relation between sample noise and image noise matrices are given by

$$X = F \tilde{\boldsymbol{\Psi}} F^H \quad (24)$$

This variance is minimized for each pixel using the Lagrangian multipliers, using the constraint in Eq. (19) yielding the SENSE solution

$$F = (E^H \tilde{\boldsymbol{\Psi}}^{-1} E)^{-1} E^H \tilde{\boldsymbol{\Psi}}^{-1} \quad (25)$$

### 3.4 Cartesian SENSE

In the standard cartesian sampling, k-space is undersampled with a reduction factor  $R$  in the Fourier domain and aliased reduced FOV image  $\hat{\rho}'_i$  is obtained in the spatial domain for each of the  $n_c$  array coils. Each pixel in the aliased image contains the local coil sensitivity weighted by signal contribution from the  $R$  pixels in the original full-FOV image  $\rho$ . From Fig. 4, it is clear that the contributing pixel positions form a cartesian grid corresponding to the size of the reduced FOV.

To reconstruct the full-FOV image  $\hat{\rho}$ , one must undo the signal superposition underlying the fold-over effect Fig. 3. The SENSE reconstruction process is sketched in Fig. 5.

The time and space complexity of Eq. (27) is reduced using cartesian SENSE. From Eq. (15), it is clear that value of each aliased pixel is a linear combination of

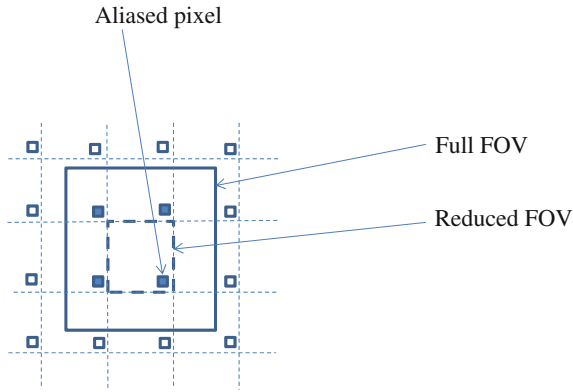


Fig. 4 Aliasing in 2D cartesian sampling

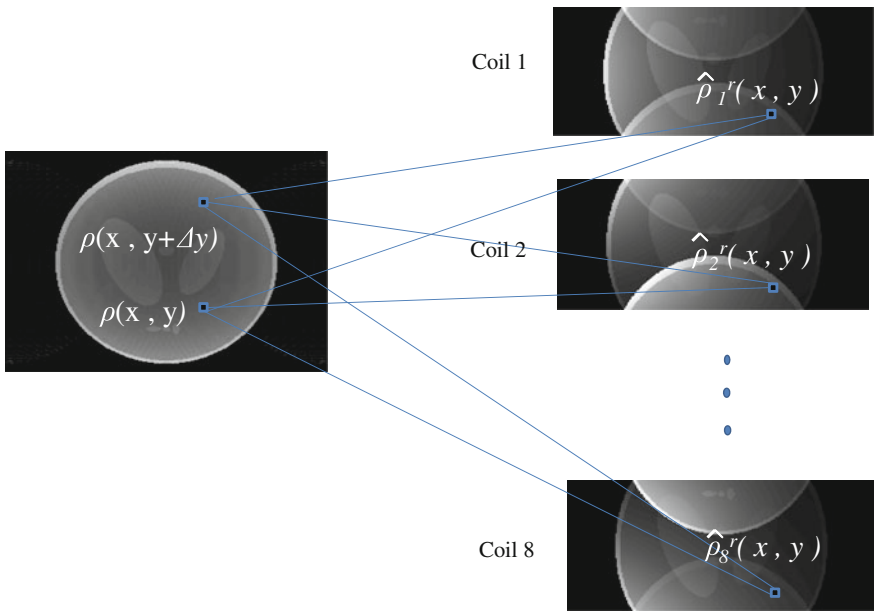
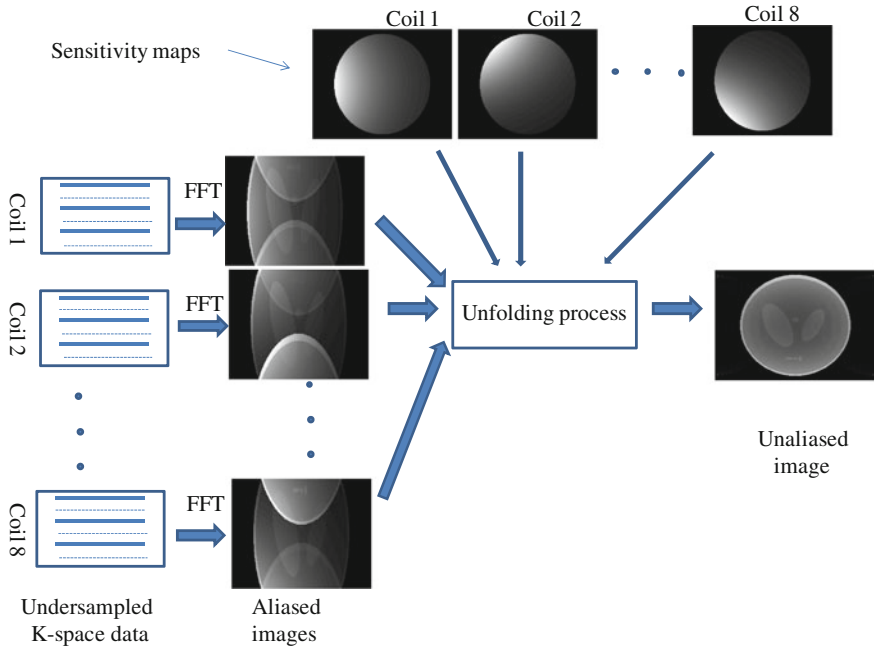


Fig. 5 Fold over in SENSE

$R$  pixel values. Therefore, the encoding matrix  $E$  becomes block diagonal. Let  $\rho_l^{r(i)}, C_l^{(i)}, \rho^{(i)}$  represent the  $i$ th column of  $\rho_l^r, C_l$ , and  $\rho$  respectively. Each column consists of  $R$  blocks. Each block represents a partitioning of signals into  $R$  aliasing components under cartesian sampling.



**Fig. 6** The SENSE process

$$\rho^{(i)} = \begin{bmatrix} \rho_1^{(i)} \\ \rho_2^{(i)} \\ \vdots \\ \rho_R^{(i)} \end{bmatrix}, \quad C_l^{(i)} = \begin{bmatrix} C_{l,1}^{(i)} \\ C_{l,2}^{(i)} \\ \vdots \\ C_{l,R}^{(i)} \end{bmatrix} \quad (26)$$

As illustrated in (Fig. 6), the  $j$ th element of  $r$ th block ( $r = 1, \dots, R$ ) of the  $i$ th column of image  $\rho$  is given by

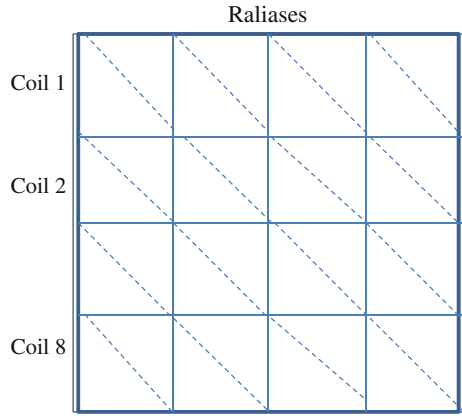
$$\rho_r^{(i)}(j) = \rho^{(i)}\left(\frac{N_{pe}}{R} \times (r-1) + j\right), \quad \text{where } j = 1, \dots, \frac{N_{pe}}{R} \quad (27)$$

The corresponding element of sensitivity vectors for each coil  $l \in \{1, \dots, n_c\}$  are given by

$$C_{l,r}^{(i)}(j) = C_l^{(i)}\left(\frac{N_{pe}}{R} \times (r-1) + j\right), \quad \text{where } j = 1, \dots, \frac{N_{pe}}{R} \quad (28)$$

$\text{diag}(C_{l,r}^{(i)})$  represents a diagonal matrix of size  $\frac{N_{pe}}{R} \times \frac{N_{pe}}{R}$ . These diagonal matrices from one column are now cascaded to form a  $\frac{N_{pe}}{R} \times N_{pe}$  matrix representation of the

Fig. 7 R aliases in SENSE



$i$ th column in the  $l$ th coil. The encoding matrix elements of the  $l$ th coil  $E_l$  is now constructed by cascading the above diagonal matrix blocks of size  $\frac{N_{pe}}{R} \times N_{pe}$  corresponding to all the columns. The stack representing each coil is now cascaded row-wise to form the encoding matrix  $E$ ,

$$E = \{E_l^r\} \quad \text{where } r = 1, \dots, R \quad (29)$$

$$l = 1, \dots, n_c$$

This is depicted in Fig. 7.

The inversion of each block corresponding to each pixel can be done independently. The encoding process given by Eq. (17) is then simplified to

$$\rho_l^r(x, y) = \sum_{m=0}^{R-1} \rho(x, y \bmod \frac{N_{pe}}{R} + m \times \frac{N_{pe}}{R}) \times C_l(x, y \bmod \frac{N_{pe}}{R} + m \times \frac{N_{pe}}{R}) \quad (30)$$

In matrix form, this becomes

$$\begin{pmatrix} \hat{\rho}_1^r(x, y) \\ \hat{\rho}_2^r(x, y) \\ \vdots \\ \hat{\rho}_{n_c}^r(x, y) \end{pmatrix} = \begin{pmatrix} C_1(x, y), C_1(x, y + N_{pe}/R), \dots, C_1(x, y + (R - 1)N_{pe}/R) \\ C_2(x, y), C_2(x, y + N_{pe}/R), \dots, C_2(x, y + (R - 1)N_{pe}/R) \\ \vdots \\ C_{n_c}(x, y), C_{n_c}(x, y + N_{pe}/R), \dots, C_{n_c}(x, y + (R - 1)N_{pe}/R) \end{pmatrix}$$

$$\begin{pmatrix} \rho(x, y) \\ \rho(x, y + N_{pe}/R) \\ \vdots \\ \rho(x, y + (R - 1)N_{pe}/R) \end{pmatrix} \quad (31)$$

where  $N_{pe} \cdot N_{fe}$  is the FOV size in pixels,  $x = 1, \dots, N_{fe}$  and  $y = 1, \dots, \frac{N_{pe}}{R}$

When the  $c = \begin{pmatrix} C_1(x, y), C_1(x, y + N_{pe}/R), \dots, C_1(x, y + (R-1)N_{pe}/R) \\ C_2(x, y), C_2(x, y + N_{pe}/R), \dots, C_2(x, y + (R-1)N_{pe}/R) \\ \vdots \\ C_{n_c}(x, y), C_{n_c}(x, y + N_{pe}/R), \dots, C_{n_c}(x, y + (R-1)N_{pe}/R) \end{pmatrix}$  matrix is non-singular for all  $x$  and  $y$ , the reconstruction problem will not be ill posed. The unfolding matrix  $U$  is then given by

$$U = (c^H \psi^{-1} c)^{-1} c^H \psi^{-1} \quad (32)$$

Therefore, the  $R$  reconstructed pixels in vector form is given by

$$\begin{pmatrix} \hat{\rho}(x, y) \\ \hat{\rho}(x, y + N_{pe}/R) \\ \vdots \\ \hat{\rho}(x, y + (R-1)N_{pe}/R) \end{pmatrix} = U \begin{pmatrix} \hat{\rho}_1^r(x, y) \\ \hat{\rho}_2^r(x, y) \\ \vdots \\ \hat{\rho}_{n_c}^r(x, y) \end{pmatrix} \quad (33)$$

### 3.5 SENSE for Optimum SNR Imaging

Parallel acquisition techniques suffer from loss in SNR when compared with optimum array imaging. In general, the SNR in the parallel MR reconstructed image is decreased by the square root of the reduction factor  $R$  as well as by an additional coil geometry dependent factor-geometry factor (g-factor) [30–32]. In SENSE, the loss in SNR arises due to ill-conditioning of the matrix inverse in SENSE reconstruction, and depends on the acceleration rate, the number of coils, and coil geometry. This loss can be explained through additional constraints imposed on the choice of array weighting factors. In standard array coil imaging, weighting factors are chosen to maximize SNR at a given point  $P$ . SENSE reconstruction has the same requirement, but in addition to that, SNR has to be minimized at a number of points  $P$ . The ultimate sensitivity limit for SENSE reconstruction can be calculated from sensitivity maps for optimum SNR imaging.

## 4 Conclusion

This approach of parallel MRI, the under-sampled MR data acquired with a set of phased-array detection coils are combined using reconstruction techniques. In SENSE, the spatial sensitivity information of the coil array needs to be determined for spatial encoding. It is very important that the calculated sensitivities are



accurate, otherwise can result in aliasing artifacts. Apart from this, parallel acquisition techniques suffer from loss in SNR when compared with optimum array imaging. All these factors need to be well addressed for optimum reconstruction in parallel MRI.

## References

1. Zhu, H.: *Medical Image Processing Overview*. University of Calgary
2. Ra, J.B., Rim, C.Y.: Fast imaging using subencoding data sets from multiple detectors. *Magn. Reson. Med.* **30**(1), 142–145 (1993)
3. Sodickson, D.K., Manning, W.J.: Simultaneous acquisition of spatial harmonics (SMASH): fast imaging with radiofrequency coil arrays. *Magn. Reson. Med.* **38**(4), 591–603 (1997)
4. Pruessmann, K., Weiger, M., Scheidegger, M., Boesiger, P.: SENSE: sensitivity encoding for fast MRI. *Mag. Res. Med.* **42**, 952–962 (1999)
5. Kyriakos, W.E., Panych, L.P., Kacher, D.F., Westin, C.F., Bao, S.M., Mulkern, R.V., Jolesz, F.A.: Sensitivity profiles from an array of coils for encoding and reconstruction in parallel (SPACE RIP). *Magn. Reson. Med.* **44**(2), 301–308 (2000)
6. Griswold, M.A., Jakob, P.M., Nittka, M., Goldfarb, J.W., Haase, A.: Partially parallel imaging with localized sensitivities (PILS). *Magn. Reson. Med.* **44**(4), 602–609 (2000)
7. McKenzie, C.A., Yeh, E.N., Sodickson, D.K.: Improved spatial harmonic selection for SMASH image reconstructions. *Magn. Reson. Med.* **46**(4), 831–836 (2001)
8. Sodickson, D.K., McKenzie, C.A.: A generalized approach to parallel magnetic resonance imaging. *Med. Phys.* **28**(8), 1629–1643 (2001)
9. Griswold, M.A., Jakob, P.M., Heidemann, R.M., Nittka, M., Jellus, V., Wang, J., Kiefer, B., Haase, A.: Generalized autocalibrating partially parallel acquisitions (GRAPPA). *Magn. Reson. Med.* **47**(6), 1202–1210 (2002)
10. Bydder, M., Larkman, D.J., Hajnal, J.V.: Generalized SMASH imaging. *Magn. Reson. Med.* **47**, 160–170 (2002)
11. Lauterbur, P.C.: Image formation by induced local interactions: examples employing nuclear magnetic resonance. *Nature* **242**, 190–191 (1973)
12. Mansfield, P., Grannell, P.K.: NMR ‘diffraction’ in solids. *J. Phys. C: Solid State Phys.* **6**(22) (1973)
13. Glover, G.H., Pelc, N.J.: A rapid-gated cine MRI technique. *Magn. Reson. Annual* (1988)
14. Ehman, R.L., Felmlee, J.P.: Adaptive technique for high-definition MR imaging of moving structures. *Radiology* **173**(1), 255–263 (1989)
15. Bloomgarden, D.C., Fayad, Z.A., Ferrari, V.A., Chin, B., Sutton, M.G., Axel, L.: Global cardiac function using fast breath-hold MRI: validation of new acquisition and analysis techniques. *Magn. Reson. Med.* **37**(5), 683–692 (1997)
16. Carlson, J.W.: An algorithm for NMR imaging reconstruction based on multiple RF receiver coils. *J. Magn. Reson.* **74**(2), 376–380 (1987)
17. Hutchinson, M., Raff, U.: Fast MRI data acquisition using multiple detectors. *Magn. Reson. Med.* **6**(1), 87–91 (1988)
18. Schenck, J.F., Hart, H.R., Foster, T.H., Edelstein, W.A., Bottomley, P.A., Hardy, C.J., Zimmerman, R.A., Bilaniuk, L.T.: Improved MR imaging of the orbit 1.5T with surface coils. *Am. J. Neuroradiol.* **6**, 193–196 (1985)
19. Hyde, J.S., Jesmanowicz, A., Gristand, T.M., Froncisz, W., Kneeland, J.B.: Quadrature detection surface coil. *Magn. Reson. Med.* **4**, 179–184 (1987)
20. Roemer, P.B., Edelstein, W.A., Hayes, C.E., Souza, S.P., Mueller, O.M.: The NMR phased array. *Magn. Reson. Med.* **16**(2), 192–225 (1990)

21. Wright, S.M., Wald, L.L.: Theory and application of array coils in MR spectroscopy. *NMR Biomed.* **10**(8), 394–410 (1997)
22. Steckner, M.C.: Advances in MRI equipment design, software, and imaging procedures. Hitachi Medical Systems America, Inc. AAPM (2006)
23. Kelton, J.R., Magin, R.L., Wright, S.M.: An algorithm for rapid image acquisition using multiple receiver coils. In: Proceedings of the SMRM 8th Annual Meeting, Amsterdam, pp. 1172 (1989)
24. Sodickson, D.K., Griswold, M.A., Edelman, R.R., Manning, W.J.: Accelerated spin echo and gradient echo imaging in the abdomen and thorax using simultaneous acquisition of spatial harmonics (SMASH). In: Proceedings of the ISMRM Annual Meeting, Vancouver, Canada, Abstract 1818 (1997)
25. Jakob, P.M., Griswold, M.A., Edelman, R.R., Sodickson, D.K.: AUTO-SMASH: a self-calibrating technique for SMASH imaging. Simultaneous acquisition of spatial harmonics. *MAGMA* **7**(1), 42–54 (1998)
26. Heidemann, R.M., Griswold, M.A., Haase, A., Jakob, P.M.: VD-AUTO-SMASH imaging. *Magn. Reson. Med.* **45**(6), 1066–1074 (2001)
27. Wang, J., Kluge, T., Nittka, M., Jellus, V., Kühn, B., Kiefer, B.: Parallel acquisition techniques with modified SENSE reconstruction mSENSE. In: First International Workshop on Parallel MRI, Wurzburg, Germany, p. 398 (2001)
28. Yanasak, N., Clarke, G., Stafford, R.J., Goerner, F., Steckner, M., Bercha, I., Och, J., Amuroa, M.: Parallel Imaging in MRI: Technology, Applications, and Quality Control, American Association of Physicists in Medicine (2015)
29. Qu, P., Zhang, B., Luo, J., Wang, J., Shen, G.X.: Improved iterative non-cartesian SENSE reconstruction using inner-regularization. In: Proceedings of the ISMRM 14, Seattle (2006)
30. Ali, A.S., Hussien, A.S., Tolba, M.F., Youssef, A.H.: Visualization of large time-varying vector data. In: 3rd IEEE International Conference on Computer Science and Information Technology, Art no. 5565176, pp. 210–215 (2010)
31. Breuer, F.A., Kannengiesser, A.R.S., Blaimer, M., Seiberlich, N., Jakob, P.M., Griswold, M. A.: General formulation for quantitative G-factor calculation in GRAPPA Reconstructions. *Magn. Reson. Med.* **62**, 739–746 (2009)
32. Ohliger, M.A., Sodickson, D.K.: An introduction to coil array design for parallel MRI. *NMR Biomed.* **19**, 300–315 (2006)